

A Novel Vanadosilicate with Hexadeca-Coordinated Cs⁺ Ions as a Highly Effective Cs⁺ Remover**

Shuvo Jit Datta, Won Kyung Moon, Do Young Choi, In Chul Hwang, and Kyung Byung Yoon*

Abstract: The effective removal of ¹³⁷Cs⁺ ions from contaminated groundwater and seawater and from radioactive nuclear waste solutions is crucial for public health and for the continuous operation of nuclear power plants. Various ¹³⁷Cs⁺ removers have been developed, but more effective ¹³⁷Cs⁺ removers are still needed. A novel microporous vanadosilicate with mixed-valence vanadium (V⁴⁺ and V⁵⁺) ions is now reported, which shows an excellent ability for Cs⁺ capture and immobilization from groundwater, seawater, and nuclear waste solutions. This material is superior to other known materials in terms of selectivity, capacity, and kinetics, and at very low Cs⁺ concentrations, it was found to be the most effective material for the removal of radioactive Cs⁺ ions under the test conditions. This novel vanadosilicate also contains hexadeca-coordinated Cs⁺ ions, which corresponds to the highest coordination number ever described.

Among various radioactive nuclides, ¹³⁷Cs is the most dangerous radioactive nuclide because of its high fission yield (6.09 %), medium half-life (30.17 years), and the very high solubility of its salts in water.^[1,2] Therefore, when accidentally released to the ground and sea, it must be immediately captured for public safety. Also, the ¹³⁷Cs⁺ ions must be effectively removed from nuclear waste solutions in the reprocessing plants for spent fuel to ensure the continuous operation of the reprocessing plants and the nuclear power plants. However, these issues have been rather challenging because the concentrations of the ¹³⁷Cs ions are usually incomparably lower (<0.1 %) than those of the co-existing competing cations (Na⁺, Ca²⁺, Mg²⁺, K⁺, and others).

Accordingly, various inorganic Cs⁺ removers have been developed.^[3–20] Among them, titanosilicates (also named crystalline silicotitanate (CST)),^[3–6] aluminosilicate zeolites, such as chabazite (CHA), clinoptilolite (HEU), and mordenite (MOR), Na⁺-exchanged phlogopite mica (Na-PMica),^[8] gallium antimony sulfide [(CH₃)₂NH₂]₂Ga₂Sb₂S₇·H₂O (GaSbS),^[10] and manganese tin sulfide K_{2x}Mn_xSn_{3–x}S₆ (x = 0.5–0.95; KMS-1)^[11,12] have received the most attention because of their high Cs⁺ removal activities. In the case of CST, there are two types of materials, that is, the original material with an ideal composition of Na₂Ti₂O₃SiO₄·2H₂O (Na-CST) and the further optimized material, which was licensed by UOP. Although the latter (UOP-CST) is currently being used at Fukushima for Cs⁺ removal from the seawater, its composition and structure are not available. For the original CST, the protonated form (H-CST) has been shown to be more active than Na-CST.

The performance of Cs⁺ removers is often compared in terms of their distribution coefficient *K_d* (in mL g^{−1}), which is the ratio of the removed amount of Cs⁺ ions per amount of the Cs⁺ remover (in g) to the amount of residual Cs⁺ ions per mL of solution [Eq. (1)]:

$$K_d = \frac{(C_i - C_f) V}{C_f m} \quad (1)$$

where *C_i* and *C_f* are the initial and final concentrations of the Cs⁺ ions, *V* is the volume of the solution in mL, and *m* is the weight of the sorbent in g.

Among the aforementioned sorbents, H-CST has shown the highest *K_d* values regardless of the type of target solution, and hence has been the best Cs⁺ remover for all purposes.^[3,17] However, no new and superior Cs⁺ removers have been developed for the last 20 years. We herein report a novel porous vanadosilicate material (named Sogang University-45, SGU-45) with *K_d* values that are much higher than that of H-CST, for *C_i* values from 10 ppb to 100 ppm. In this work, H-CST and Na-CST refer to the original CST material and not to the UOP-CST remover.

We first synthesized parent vanadosilicates, which are denoted as Na_xCs_y-SGU-4 (x + y = 7, 3 ≤ x ≤ 7, 0 ≤ y ≤ 4) (Figure 1 a–e; see also the Supporting Information, Section S1). Their electron diffraction patterns are shown in Figure 1 f–j (see also Figures S2–S6), and schematic illustrations of their shapes and the corresponding crystal axes are shown in Figure 1 k–o. The corresponding powder diffraction patterns are shown in Figure S7. The crystals grew longer along the *c* axis with an increase in the Cs⁺ content of the gel.

The crystal structures of Na₇Cs₀V₄Si₁₂O₃₆·xH₂O (*P*4̄m2; Figure 1 a)^[21] and Na₄Cs₃V₄Si₁₂O₃₆·xH₂O (*P*4̄m2; Figure 1 e)

[*] Dr. S. J. Datta, W. K. Moon, D. Y. Choi, Prof. Dr. I. C. Hwang, Prof. Dr. K. B. Yoon
Korea Center for Artificial Photosynthesis
Center for Nanomaterials, Department of Chemistry
Sogang University, Seoul 121-742 (Korea)
E-mail: yoonkb@sogang.ac.kr

[**] This work was supported by the Ministry of Science, ICT and Future Planning through the National Research Foundation of Korea (2012R1A2A3A01009806). X-ray crystallography data was collected from a synchrotron radiation beamline (PLS-II 2D-SMC) at Pohang Accelerator Laboratory, Korea. We thank Dr. Dohyun Moon (Supramolecule/Small molecule Crystallography) at Pohang Accelerator Laboratory, Korea for his great help in obtaining diffraction data. We also thank Jiyun Lee for her help in drawing Figure 1 and Hwang Byung Yoon for his help in supplying seawater. Sogang University has filed patents on the results presented here (Application numbers: PCT/KR2014/001659 and 10-2014-0024439). I.C.H. is grateful for a Sogang University Research Grant (201110032).

Supporting information for this article is available on the WWW under <http://dx.doi.org/10.1002/anie.201402778>.

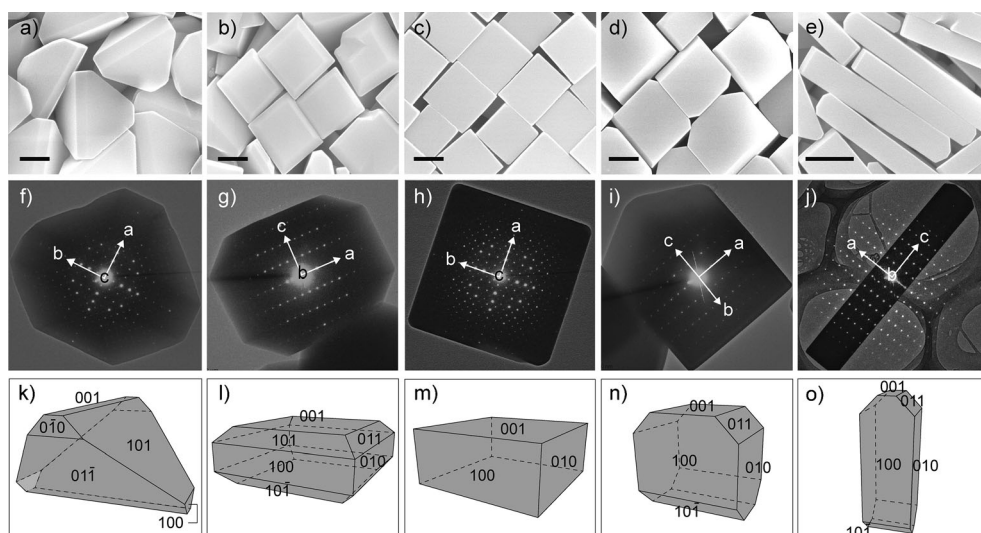


Figure 1. Morphology of $\text{Na}_x\text{Cs}_{7-x}\text{SGU-4}$. a–e) SEM images of $\text{Na}_x\text{Cs}_{7-x}\text{SGU-4}$ crystals synthesized from gels with different molar ratios of CsCl (0.43, 1.30, 1.95, 2.60, and 4.55 with respect to V). Scale bars: 500 nm. f–j) Overlaid images obtained by low-resolution transmission electron microscopy (TEM) and corresponding electron diffraction patterns for the crystals shown above. k–o) Schematic illustrations of the crystal shapes of $\text{Na}_x\text{Cs}_{7-x}\text{SGU-4}$ showing various percentages of the {100}, {010}, {0 $\bar{1}$ 0}, {011}, {0 $\bar{1}$ $\bar{1}$ }, {101}, {10 $\bar{1}$ }, and {001} facets.

were obtained with a synchrotron radiation diffractometer (Figures S8 and S9 and Tables S1–S3). Their unit cell formulas can be represented as $\text{Na}_7[(\text{SBU-A})(\text{SBU-B})_2] \cdot x\text{H}_2\text{O}$ (denoted as $\text{Na}_7\text{-SGU-4}$) and $\text{Na}_4\text{Cs}_3[(\text{SBU-A})(\text{SBU-B})_2] \cdot x\text{H}_2\text{O}$ (denoted as $\text{Na}_4\text{Cs}_3\text{-SGU-4}$), respectively, in terms of the secondary building units A (SBU-A) and B (SBU-B), where $\text{SBU-A} = \text{Si}_{12}\text{O}_{32}[\text{Cs}(\text{H}_2\text{O})_4]$ and $\text{SBU-B} = (\text{V}=\text{O})_2\text{H}_2\text{O}$. The oxidation state of vanadium is +4 (Figures S10 and S11). Raman spectroscopy confirmed the presence of $\text{V}=\text{O}$ groups (Figure S12). The cell parameters are $a = 11.533(2) \text{ \AA}$, $c = 7.837(2) \text{ \AA}$, and $V = 1042.4(4) \text{ \AA}^3$ for $\text{Na}_7\text{-SGU-4}$ and $a = 11.545(2) \text{ \AA}$, $c = 7.835(2) \text{ \AA}$, and $V = 1044.1(4) \text{ \AA}^3$ for $\text{Na}_4\text{Cs}_3\text{-SGU-4}$. The chemical compositions, unit cell formulas, and the Na^+/Cs^+ ratios for the crystals shown in Figure 1 b–e are given in Table S4.

The structures of the SBUs, the interconnection pattern, and the unit cell structures are shown in Figure 2. SBU-A consists of a non-exchangeable Cs^+ ion, a twelve-membered oxygen ring, which is folded into a U shape, and four water molecules (Figure 2b). Its polyhedron and ORTEP representations are shown in Figure 2c. The van der Waals distances are 3.383 \AA between the Cs^+ ion and the eight O(2) atoms, 3.590 \AA between the Cs^+ ion and the four O(5) atoms, and 4.793 \AA between the Cs^+ ion and the four oxygen atoms of the four water molecules (Table S3). They are shorter than the sum (4.95 \AA) of the van der Waals radii of cesium (3.43 \AA) and oxygen (1.52 \AA),^[22] indicating that the Cs^+ ions are hexadeca-coordinated (Figure S13), which is higher than the highest coordination number ever observed with Cs^+ (12).^[23] This value is even higher than the highest coordination number (14) that has ever been observed for any metal center.^[24,25] The extremely short $\text{Cs}^+-\text{O}(2)$ and $\text{Cs}^+-\text{O}(5)$ distances indicate that these bonds are extraordinarily strong.

SBU-A readily undergoes linkage formation along the c axis, forming a silica tube packed with $[\text{Cs}(\text{H}_2\text{O})_4]^+$ ions (Figure 2d). This creates two pairs of confronting eight-membered O rings. A view of the silica tube along the c axis and the corresponding perspective view show that it is a square silica tube (Figure 2e,f). Each square silica tube is interconnected to the neighboring one through two SBU-B units. The SBU-B unit can be viewed as a unit of two V^{4+} octahedra that are linked through a corner-sharing oxygen atom and capped by a water molecule (Figure 2g,h). As the direction of the $\text{H}_2\text{O}-\text{V}=\text{O}-\text{V}=\text{O}$ chain is randomly oriented, the positions of the

V^{4+} centers are crystallographically disordered (Figure 2h). The $\text{H}_2\text{O}-\text{V}=\text{O}-\text{V}=\text{O}$ unit can also be viewed as the shortest one-dimensional -V-O-V-O- quantum wire of the related vanadosilicate AM-6.^[26,27]

Views of the $\text{Na}_7\text{-SGU-4}$ structure along the c and b axes are shown in Figure 2i and 2j, respectively. Another eight-membered ring exists at the center of four square silica tubes, and a six-membered ring exists between the two square silica tubes. The non-framework sites for the Cs^+ ions are denoted as I, II, and III (Figure 2k). In $\text{Na}_4\text{Cs}_3\text{-SGU-4}$, the Cs^+ occupancies are 50 %, 50 %, and 20 % for I, II, and III, respectively. The views along the c and b axes are shown in Figure 2l, m.

The Na^+ ions in $\text{Na}_7\text{-SGU-4}$ are not exchangeable with Cs^+ ions. Interestingly, however, a partial oxidation of the V^{4+} ions to V^{5+} ions triggers its capability for Cs^+ ion exchange. Therefore, we prepared a partially (60 %) oxidized form, namely $\text{Na}_{4.6}[(\text{SBU-A})\{(\text{V}^{4+})_{0.4}(\text{V}^{5+})_{0.6}\}(\text{SBU-B})_2] \cdot x\text{H}_2\text{O}$, by treating the precursor with an appropriate amount of Br_2 (Section S14). This oxidized form is denoted as $\text{Na}_{4.6}\text{-SGU-45}$. The Na^+ ions in $\text{Na}_{4.6}\text{-SGU-45}$ were subsequently fully ion-exchanged with K^+ ions to give $\text{K}_{4.6}\text{-SGU-45}$ (denoted as K-SGU-45) because we found that K^+ ions were more easily replaced by Cs^+ ions.

In the above, the strikingly different behaviors of $\text{Na}_7\text{-SGU-4}$ and $\text{Na}_{4.6}\text{-SGU-45}$ with respect to their Cs^+ ion exchange capability seemed to arise from the fact that the binding between the framework oxygen atoms of $\text{Na}_7\text{-SGU-4}$ and the Na^+ ions is much stronger than that between the framework oxygen atoms of $\text{Na}_{4.6}\text{-SGU-45}$ and the Na^+ ions because of a much higher negative charge density on the framework oxygen atoms in $\text{Na}_7\text{-SGU-4}$ than in $\text{Na}_{4.6}\text{-SGU-45}$. Thus, strong binding between the framework and the

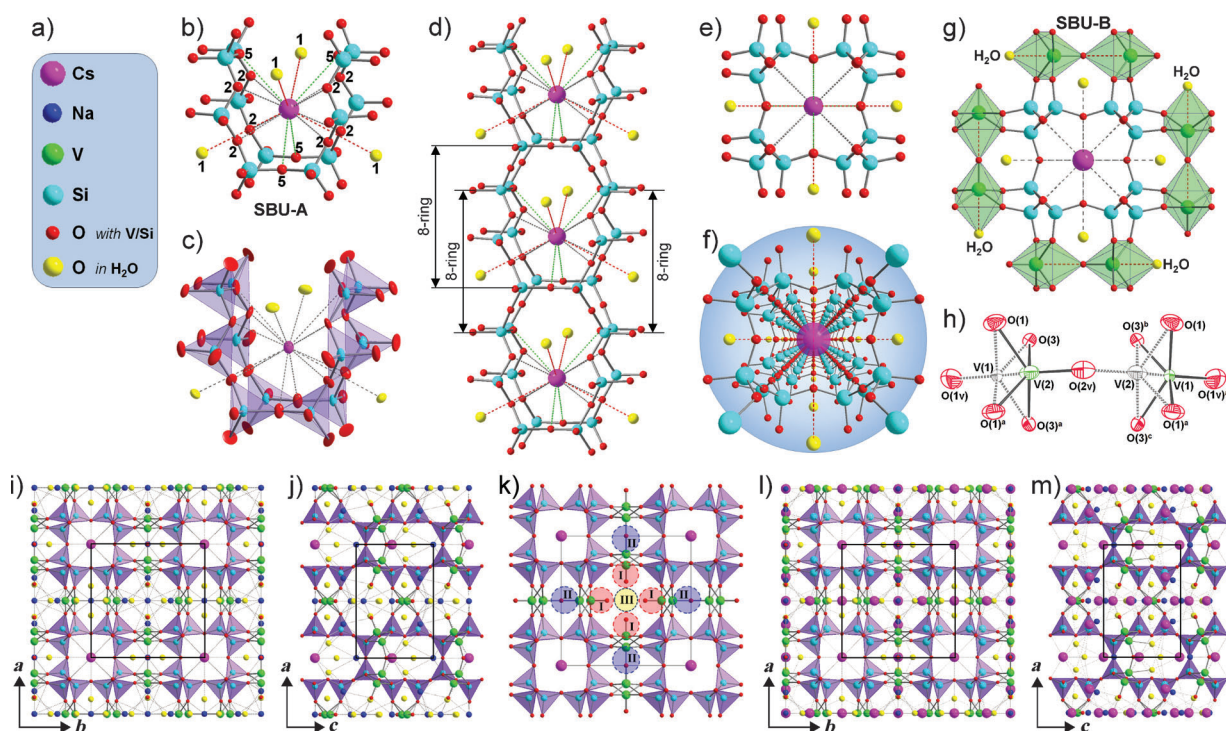


Figure 2. Framework structures and secondary building units (SBU) of $\text{Na}_7\text{-SGU-4}$ and $\text{Na}_4\text{Cs}_3\text{-SGU-4}$. a) Color labelling scheme. b) Structure of SBU-A, which consists of a twelve-membered oxygen ring and a $[\text{Cs}(\text{H}_2\text{O})_4]^+$ unit. c) Polyhedron and ORTEP representations of SBU-A. d) The linkage of SBU-A units along the c axis leads to a silica tube packed with $[\text{Cs}(\text{H}_2\text{O})_4]^+$ units, creating eight-membered O rings. e) Square silica tube viewed along the c axis. f) Perspective view of a square silica tube along the c axis. g) View of SBU-B units and their connectivity to SBU-A. h) Disordered positions of vanadium in SBU-B units. i, j) Unit-cell structure of $\text{Na}_7\text{-SGU-4}$ viewed along the c and b axes, respectively. k) Three sites for the exchangeable Cs^+ ions in $\text{Na}_4\text{Cs}_3\text{-SGU-4}$. l, m) Unit-cell structure of $\text{Na}_4\text{Cs}_3\text{-SGU-4}$ viewed along the c and b axes, respectively.

Na^+ ions gives rise to poor mobility of the Na^+ ions. In support of this explanation, we reported the presence of V^{4+} -to-O metal-to-ligand charge transfer in AM-6 (the related vanadosilicate with all V^{4+} framework ions),^[27] which gives rise to an increase in the negative charge density of the framework oxygen atoms, and Cygan, Ockwig, Nenoff, and co-workers have shown that an increase in the negative charge density of the framework oxygen atoms gives rise to an increase in the binding strength between the framework oxygen atoms and the charge-balancing cation.^[28,29]

Using simulated groundwater (Na^+ : 125, Ca^{2+} : 24, Mg^{2+} : 9, K^+ : 6 ppm), the Cs^+ ion removal capacities of K-SGU-45, H-CST, Na-CST, Na-PMica, CHA, and GaSbS were measured. Among the six reference samples, H-CST, Na-CST, Na-PMica, and GaSbS were prepared according to previously reported procedures (Section S15).^[4,6,8,10,30] All samples were used in the binder-free powder forms (Figure S16). First, these samples were evaluated under conditions where the total number of Cs^+ ions in solution was adjusted to be the same as the total number of exchangeable sites (“one-equivalent conditions”), while the overall Cs^+ ion concentration was kept at 1.2 ppm. The amounts of the sorbents that were used under the one-equivalent conditions and at $C_i = 1.2$ ppm were 2.6, 2.2, 2.5, 2.5, 4.3, and 5.3 mg for K-SGU-45, H-CST, Na-CST, Na-PMica, CHA, and GaSbS, respectively. The time allowed for ion exchange was eight hours. As shown in Figure 3a, the degrees of ion exchange were 25, 22, 21, 7.6, 3, and 1%, respectively. The corresponding $\log K_d$ values

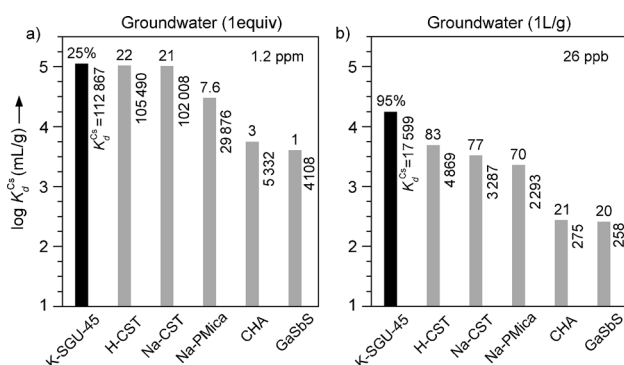


Figure 3. Cs^+ capture in simulated groundwater. Comparison of $\log K_d$, K_d , and the degree of ion exchange for K-SGU-45 and previously reported Cs^+ sorbents (as indicated) under the one-equivalent conditions with $C_i = 1.2$ ppm (a) and at 1 L g^{-1} with $C_i = 26$ ppb (b) under the described test conditions.

were determined to be 5.05, 5.02, 5.01, 4.48, 3.73, and 3.61. This result shows that the Cs^+ removal capacity of K-SGU-45 is higher than those of the five other sorbents. At a much lower concentration ($C_i = 26$ ppb) and for 1 L per 1 gram of the remover (1 L g^{-1}), K-SGU-45 showed a more pronounced performance than the other sorbents (Figure 3b).

Next, the Cs^+ removal performances were evaluated with real seawater and in a system that simulated a nuclear waste

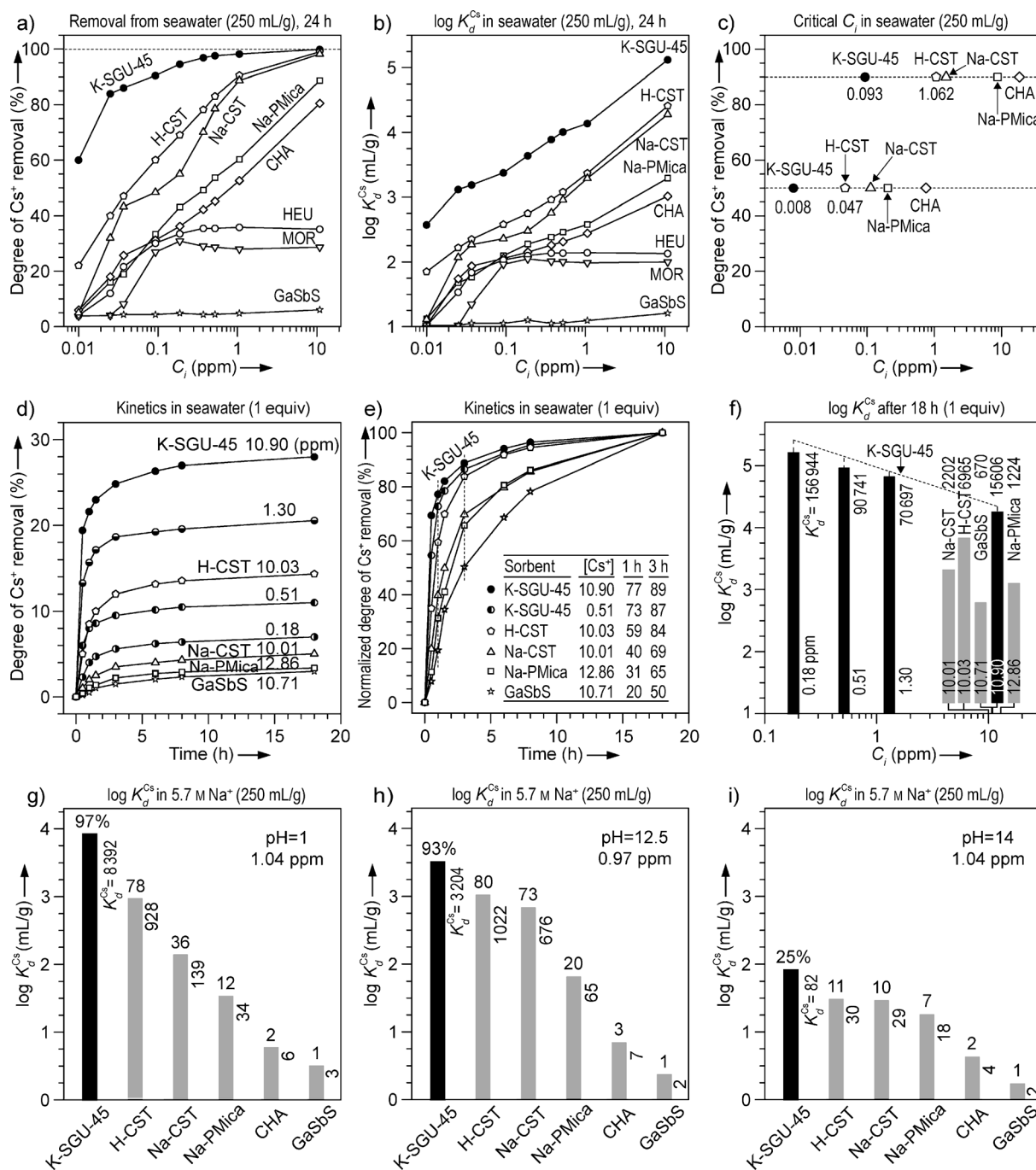


Figure 4. Cs⁺ capture in real seawater and in simulated nuclear waste solutions. a, b) Comparison of the degrees of Cs⁺ removal (a) and the corresponding $\log K_d$ values (b) for K-SGU-45 and other Cs⁺ sorbents at $V_m^{-1} = 250$ mL g⁻¹ and $0.01 \text{ ppm} \leq C_i \leq 10$ ppm in real seawater after equilibration for 24 hours. c) The critical C_i values at which the four sorbents can remove 50 and 90% of Cs⁺ ions from the seawater at $V_m^{-1} = 250$ mL g⁻¹ and $0.01 \text{ ppm} \leq C_i \leq 12$ ppm. d, e) Time profiles of the degrees (d) and the normalized degrees (e) of Cs⁺ removal from seawater at $C_i = 0.18, 0.51, 1.30$, and 10.90 ppm for K-SGU-45 and at $C_i \approx 10$ ppm for H-CST, Na-CST, Na-PMica, and GaSbS under the one-equivalent conditions. Inset: Normalized degrees of Cs⁺ removal after 1 h and 3 h for the six sorbents. f) Plot of the corresponding $\log K_d$ (K_d) values with respect to C_i . g–i) Comparison of the $\log K_d$ (K_d) values of the six sorbents obtained from the simulated nuclear waste solutions at pH 1 (g), pH 12.5 (h), and pH 14 (i) at $V_m^{-1} = 250$ mL g⁻¹ and $C_i = 1$ ppm.

solution (Figure 4). The seawater used in this study was taken from the Yellow Sea near the island Anmyeondo, which is located at the western coast of Korea. The concentrations of Na⁺, Mg²⁺, K⁺, and Ca²⁺ were determined to be 11 000, 1200, 600, 300 ppm, respectively. The degrees of Cs⁺ removal from

the real seawater for 250 mL g^{-1} and $10 \text{ ppb} \leq C_i \leq 10.9$ ppm and the corresponding $\log K_d$ – C_i plots for various sorbents are shown in Figure 4a, b. At $C_i = 10.9$ ppm, the degrees of Cs⁺ removal were 100, 99, 99, 89, 81, 35, 29, and 6% for K-SGU-45, H-CST, Na-CST, Na-PMica, CHA, HEU, MOR, and

GaSbS, respectively (Figure 4a; Tables S5–S6). The $\log K_d$ values were determined to be 5.12, 4.41, 4.29, 3.29, 3.01, 2.13, 2.00, and 1.21 mL g^{-1} , respectively (Figure 4b). The degree of Cs^+ removal decreased sharply with decreasing C_i values (Figure 4a). However, this decrease in removal efficiency was much slower for K-SGU-45 than for the other sorbents, which highlights that the performance of K-SGU-45 becomes more outstanding at low C_i concentrations.

At $C_i = 10$ ppb, the degree of Cs^+ removal by K-SGU-45 is 60%; for other sorbents, it was determined to be $\leq 22\%$ (Figure 4a). Accordingly, the $\log K_d$ value of K-SGU-45 (2.57) was higher than those of the other materials (≤ 1.85 ; Figure 4b). Thus, K-SGU-45 can be immediately employed to remediate seawater contaminated with $^{137}\text{Cs}^+$ ions. The critical Cs^+ concentrations at which the sorbents can remove 50% and 90% of the Cs^+ ions from real seawater at 250 mL g^{-1} are shown in Figure 4c. This result demonstrates that K-SGU-45 is superior to H-CST, which has been the best Cs^+ remover for the last 20 years.

Under the one-equivalent conditions in seawater, the C_i dependent and normalized kinetic profiles and the $\log K_d$ values of K-SGU-45 for C_i values between 0.18 and 10.9 ppm are shown in Figure 4d–f (see also Figure S17). The results are also compared with those of H-CST, Na-CST, Na-PMica, and GaSbS for $C_i \approx 10$ ppm. Under these one-equivalent conditions, the competition between the Cs^+ ions and co-existing cations (M^{n+}) becomes much more severe as C_i decreases. Thus, when C_i decreases by a factor of ten, the volume of seawater and the $\text{M}^{n+}/\text{Cs}^+$ ratio ($\text{M}^{n+} = \text{Na}^+, \text{Mg}^{2+}, \text{Ca}^{2+}, \text{K}^+$, etc.) increase by the same factor. As a result, the opportunity for Cs^+ ions to be taken up by a Cs^+ remover decreases also by a factor of ten. For the tested concentrations of $C_i = 10.90, 1.30, 0.51$, and 0.18 ppm, the required seawater volumes to obtain one-equivalent conditions for 1 g of K-SGU-45 are 34, 286, 726, and 2092 L, respectively. The corresponding seawater volumes for 1 g of H-CST (10.03 ppm), Na-CST (10.01 ppm), Na-PMica (12.86 ppm), and GaSbS (10.71 ppm) are 47, 42, 31, and 18 L, respectively. Thus, the competition between the Cs^+ and M^{n+} ions is much more severe under the one-equivalent conditions than at 250 mL g^{-1} . Therefore, the one-equivalent conditions represent the most suitable set-up to compare the intrinsic affinities of sorbents to Cs^+ ions.

Approximately 15 hours were required to reach full equilibrium (Figure 4d). For $C_i \approx 10$ ppm, the degrees of Cs^+ removal were 28% (K-SGU-45), 14% (H-CST), 5% (Na-CST), 4% (Na-PMica), and 3% (GaSbS), demonstrating that K-SGU-45 has an approximately 2–9 times higher affinity for Cs^+ ions than the other sorbents at relatively high C_i values (ca. 10 ppm). Interestingly, however, even at low C_i concentrations (1.3 ppm), which corresponds to 286 L of seawater per one gram of K-SGU-45, the degree of Cs^+ removal by K-SGU-45 was 21%, which is still higher than those for H-CST (47 L), Na-CST (42 L), Na-PMica (31 L), and GaSbS (18 L) at much higher C_i values (ca. 10 ppm). Simply based on the volume ratio of seawater (ca. 286 L vs ca. 47 L), the affinity of K-SGU-45 for Cs^+ ions can be regarded to be higher than that of H-CST by a factor of six. However, considering that the degree of inhibition by the competing

cations also increases by a factor of six, it may be concluded that the affinity of K-SGU-45 to Cs^+ ions exceeds that of H-CST by a factor of 36.

A comparison of the normalized Cs^+ removal profiles of K-SGU-45 at $C_i = 10.90$ and 0.51 ppm with those of H-CST, Na-CST, Na-PMica, and GaSbS at $C_i \approx 10$ ppm shows that whereas K-SGU-45 has removed 77% ($C_i = 10.90\%$) and 73% ($C_i = 0.51\%$) of the Cs^+ ions in terms of its maximum capacities after one hour, H-CST, Na-CST, Na-PMica, and GaSbS have only removed 59, 40, 31, and 20% of their maximum capacities, respectively (Figure 4e). After three hours, the removed amounts corresponded to 89, 87, 84, 69, 65, and 50% of their maximum capacities. This result clearly shows that K-SGU-45 not only has a much higher affinity to Cs^+ ions from a thermodynamic point of view, but also removes Cs^+ ions more rapidly than the other four Cs^+ sorbents. The Cs^+ removal profile of K-SGU-45 with time for a Cs^+ solution of 1.3 ppm in water and seawater with $V \text{ m}^{-1} = 1 \text{ L g}^{-1}$ shows that 95% of the Cs^+ ions were removed from the aqueous solution and more than 85% of the Cs^+ ions were removed from the seawater within ten minutes (Figure S18). This kinetic superiority is also important for the rapid remediation of contaminated seawater.

Surprisingly, in the case of K-SGU-45 under the one-equivalent conditions, K_d increases as C_i decreases (as the seawater volume increases, as the amount of the competing cations (M^{n+}) increases, or as the competition between Cs^+ and M^{n+} ions ($\text{M}^{n+}/\text{Cs}^+$ ratio) increases; Figure 4f). This is a truly remarkable unprecedented phenomenon that shows that K-SGU-45 is most suited to remove $^{137}\text{Cs}^+$ ions from contaminated seawater, in particular, when the accidentally released $^{137}\text{Cs}^+$ ions are diluted by seawater.

The removal of $^{137}\text{Cs}^+$ ions from stored highly basic nuclear waste solutions has been another big challenge. We prepared three solutions with total Na^+ concentrations of 5.7 M, but with different pH values (pH 1, 12.5, and 14). K-SGU-45 was stable under these conditions (Figure S19). For each solution with $V \text{ m}^{-1} = 250 \text{ mL g}^{-1}$, the Cs^+ removal capacities of the six sorbents were compared (Figure 4g–i). As noted, even at a Na^+ concentration of 5.7 M, the Cs^+ capturing capacity of K-SGU-45 was still superior to those of other high-performance Cs^+ capture materials, regardless of the pH value. This demonstrates that K-SGU-45 is also the most suitable material for the removal of $^{137}\text{Cs}^+$ ions from stored nuclear waste solutions.

We have reported a synthetic method for and the structure of the novel vanadosilicate K-SGU-45 and investigated its extraordinarily high capability for Cs^+ removal, which excelled those of existing materials under our test conditions. K-SGU-45 should be very useful to capture and immobilize Cs^+ ions from contaminated groundwater or seawater and highly acidic or basic nuclear waste solutions. This work will trigger the syntheses of various vanadium and other transition-metal silicates to capture various radioactive nuclides, such as $^{90}\text{Sr}^{2+}$ ions, and other toxic heavy-metal ions. Furthermore, the discovery of unprecedented hexadeca-coordinated Cs^+ centers, which corresponds to the highest coordination number ever observed in chemistry, has been described.

Received: March 2, 2014
Published online: May 22, 2014

Keywords: cesium · coordination modes · microporous materials · radioactive ions · vanadosilicate

- [1] P. C. Burns, R. C. Ewing, A. Navrotsky, *Science* **2012**, 335, 1184–1188.
- [2] N. Yoshida, J. Kanda, *Science* **2012**, 336, 1115–1116.
- [3] R. G. Anthony, R. G. Dosch, D. Gu, C. V. Philip, *Ind. Eng. Chem. Res.* **1994**, 33, 2702–2705.
- [4] D. M. Poojary, R. A. Cahill, A. Clearfield, *Chem. Mater.* **1994**, 6, 2364–2368.
- [5] A. J. Celestian, A. Clearfield, *J. Mater. Chem.* **2007**, 17, 4839–4842.
- [6] A. J. Celestian, J. D. Kubicki, J. Hanson, A. Clearfield, J. B. Parise, *J. Am. Chem. Soc.* **2008**, 130, 11689–11694.
- [7] A. I. Bortun, L. N. Bortun, D. M. Poojary, O. Xiang, A. Clearfield, *Chem. Mater.* **2000**, 12, 294–305.
- [8] S. Komarneni, R. Roy, *Science* **1988**, 239, 1286–1288.
- [9] S. Komarneni, R. Roy, *Nature* **1982**, 299, 707–708.
- [10] N. Ding, M. G. Kanatzidis, *Nat. Chem.* **2010**, 2, 187–191.
- [11] M. J. Manos, N. Ding, M. G. Kanatzidis, *Proc. Natl. Acad. Sci. USA* **2008**, 105, 3696–3699.
- [12] M. J. Manos, M. G. Kanatzidis, *J. Am. Chem. Soc.* **2009**, 131, 6599–6607.
- [13] J. L. Mertz, Z. H. Fard, C. D. Malliakas, M. J. Manos, M. G. Kanatzidis, *Chem. Mater.* **2013**, 25, 2116–2127.
- [14] D. Yang, S. Sarina, H. Zhu, H. Liu, Z. Zheng, M. Xie, S. V. Smith, S. Komarneni, *Angew. Chem.* **2011**, 123, 10782–10786; *Angew. Chem. Int. Ed.* **2011**, 50, 10594–10598.
- [15] A. Clearfield, A. I. Bortun, L. N. Bortun, D. M. Poojary, S. A. Khainakov, *J. Mol. Struct.* **1998**, 470, 207–213.
- [16] T. Möller, R. Harjula, M. Pillinger, A. Dyer, J. Newton, E. Tusa, S. Amin, M. Webb, A. Araya, *J. Mater. Chem.* **2001**, 11, 1526–1532.
- [17] T. M. Nenoff, J. L. Krumhansl, *Solvent Extr. Ion Exch.* **2012**, 30, 33–40.
- [18] K. Yoshida, K. Toyoura, K. Matsunaga, A. Nakahira, H. Kurata, Y. H. Ikuhara, Y. Sasaki, *Sci. Rep.* **2013**, 3, 2457.
- [19] H. Yeritsyan, A. Sahakyan, V. Harutyunyan, S. Nikoghosyan, E. Hakhverdyan, N. Grigoryan, A. Hovhannisyanyan, V. Atoyan, Y. Keheyanyan, C. Rhodes, *Sci. Rep.* **2013**, 3, 2900.
- [20] M. Endo, E. Yoshikawa, N. Muramatsu, N. Takizawa, T. Kawai, H. Unuma, A. Sasaki, A. Masano, Y. Takeyama, T. Kahara, *Chem. Technol. Biotechnol.* **2013**, 88, 1597–1602.
- [21] CCDC 979469 and 979470 contain the supplementary crystallographic data for this paper. These data can be obtained free of charge from The Cambridge Crystallographic Data Centre via www.ccdc.cam.ac.uk/data_request/cif.
- [22] M. Mantina, A. C. Chamberlin, R. Valero, C. J. Cramer, D. G. Truhlar, *J. Phys. Chem. A* **2009**, 113, 5806–5812.
- [23] S. P. Gromov, A. I. Vedernikov, N. A. Lobova, L. G. Kuzmina, S. S. Basok, Y. A. Strelenko, M. V. Alfimova, J. A. K. Howarde, *New J. Chem.* **2011**, 35, 724–737.
- [24] G. A. Barclay, T. M. Sabine, J. C. Taylor, *Acta Crystallogr.* **1965**, 19, 205–209.
- [25] E. R. Bernstein, W. C. Hamilton, T. A. Keiderling, S. J. L. Placa, S. J. Lippard, J. J. Mayerle, *Inorg. Chem.* **1972**, 11, 3009–3016.
- [26] J. Rocha, P. Brandao, Z. Lin, M. W. Anderson, V. Alfredsson, O. Terasaki, *Angew. Chem.* **1997**, 109, 134–136; *Angew. Chem. Int. Ed. Engl.* **1997**, 36, 100–102.
- [27] S. J. Datta, K. B. Yoon, *Angew. Chem.* **2010**, 122, 5091–5095; *Angew. Chem. Int. Ed.* **2010**, 49, 4971–4975.
- [28] N. W. Ockwig, R. T. Cygan, L. J. Criscenti, T. M. Nenoff, *Phys. Chem. Chem. Phys.* **2008**, 10, 800–807.
- [29] N. W. Ockwig, R. T. Cygan, M. A. Hartl, L. L. Daemen, T. N. Nenoff, *J. Phys. Chem. C* **2008**, 112, 13629–13634.
- [30] D. M. Poojary, A. I. Bortun, L. N. Bortun, A. Clearfield, *Inorg. Chem.* **1996**, 35, 6131–6139.